

Bimetal loaded graphitic carbon nitride with synergistic enhanced peroxidase-like activity for colorimetric detection of p-phenylenediamine

Jianshuai Mu^{a,d}, Mengjiao Ren^a, Ning Li^a, Tengyi Zhao^a, Zhong-Yi Liu^a, Jingwen Ma^a, Shulai Lei^c, Jiajun Wang^{a,*}, En-Cui Yang^{a,*}, Yan Wang^{b,*}

^a *Academy of Interdisciplinary Studies on Intelligent Molecules, College of Chemistry, Tianjin Key Laboratory of Structure and Performance for Functional Molecules, Tianjin Normal University, Tianjin 300387, China*

^b *School of Chemistry and Chemical Engineering, Harbin Institute of Technology, Harbin 150001, China*

^c *Hubei Key Laboratory of Low Dimensional Optoelectronic Materials and Devices, Hubei University of Arts and Science, Xiangyang 441053, China*

^d *Tianjin Saina Enzyme Technology Co., Ltd, Tianjin 300192, Peoples R China*

Corresponding author.

E-mail addresses: hxxywjj@tjnu.edu.cn (J. Wang), encui_yang@163.com (E.-C. Yang), wangy_msn@hit.edu.cn (Y. Wang).

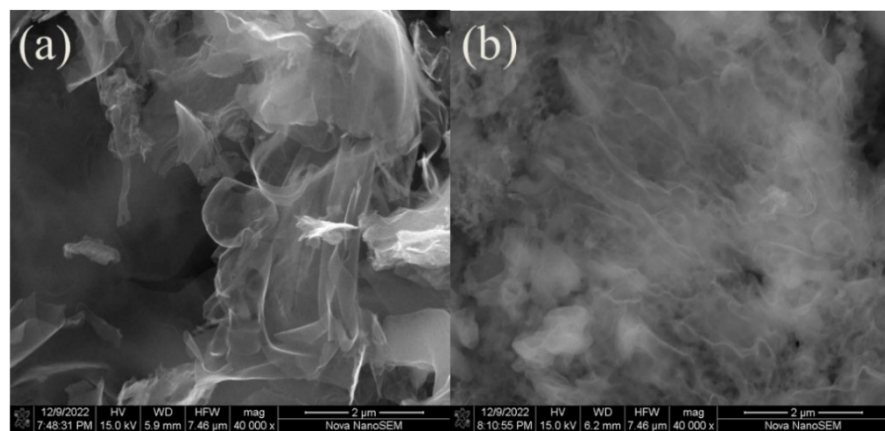


Fig. S1 (a) SEM of pristine CN and (b) Fe/Ni-CN.

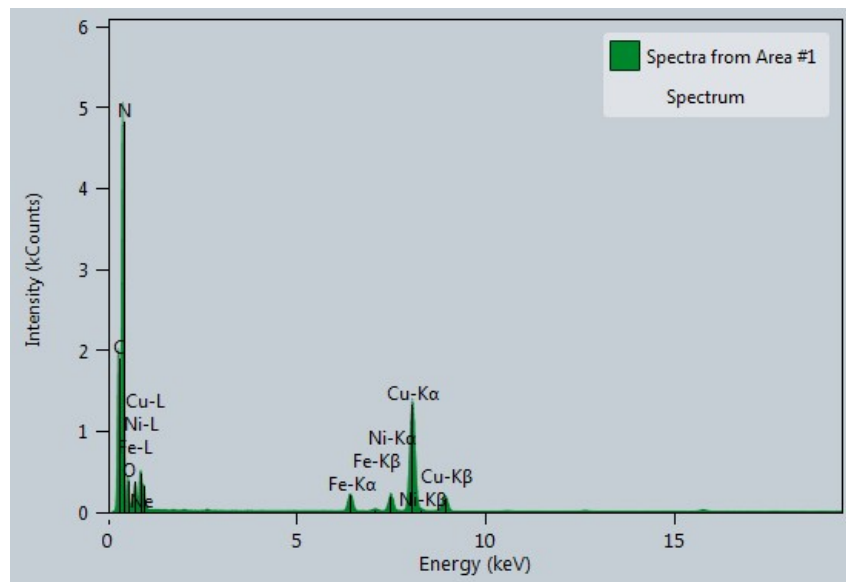


Fig. S2 EDS spectrum of Fe/Ni-CN.

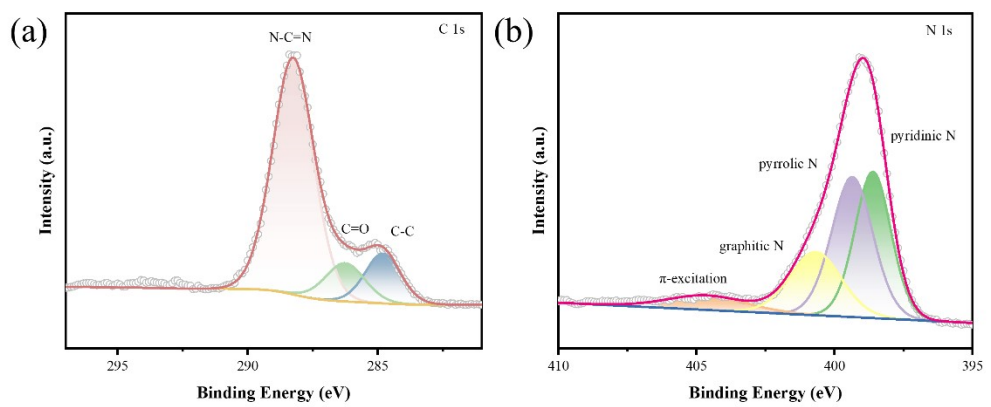


Fig. S3 XPS spectra of C 1s (a) and N 1s (b).

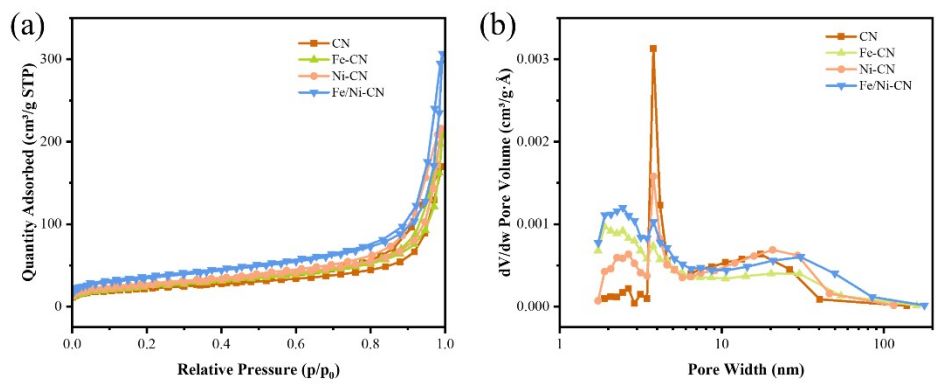


Fig. S4 (a) N₂ adsorption/desorption isotherms of CN, Fe-CN, Ni-CN and Fe/Ni-CN and (b) the corresponding pore-size distribution curves.

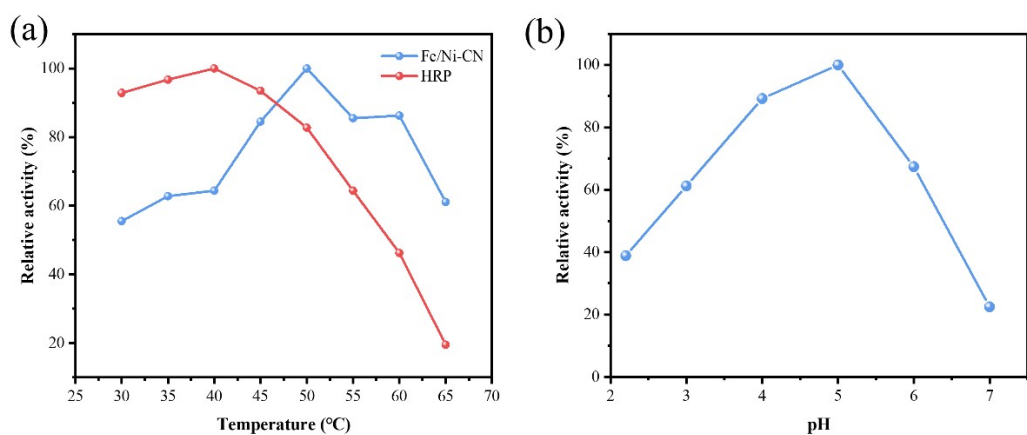


Fig. S5 (a) Comparison of Fe/Ni-CN and HRP under varying temperature, (b) The influence of pH on the catalytic activity of Fe/Ni-CN.

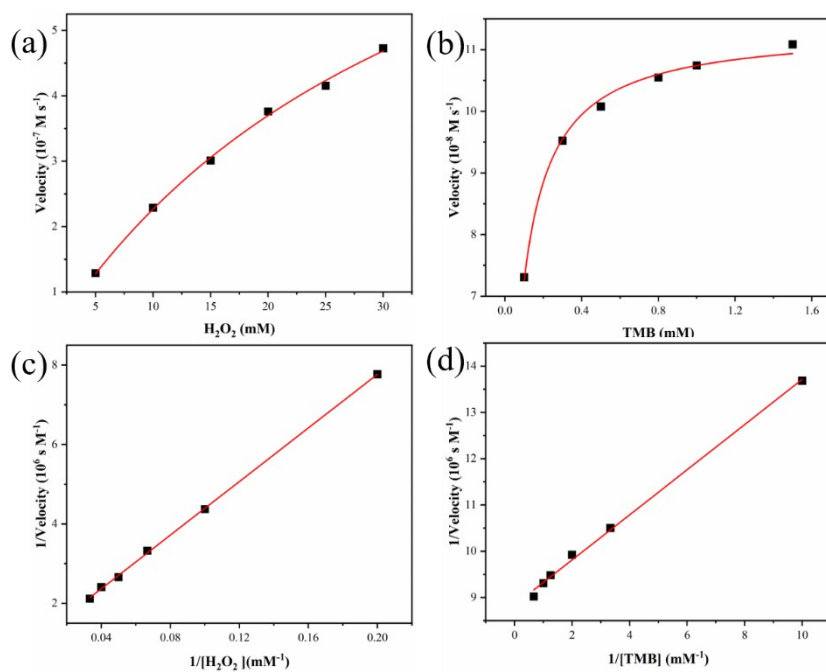


Fig. S6 Steady-state kinetics of Fe-CN nanozyme. (a and b) Michaelis–Menten curves fit for varied concentrations of H_2O_2 with fixed concentration of TMB, and varied concentrations of TMB with fixed concentration of H_2O_2 . The Lineweaver–Burk plots for various concentrations of (c) H_2O_2 and (d) TMB.

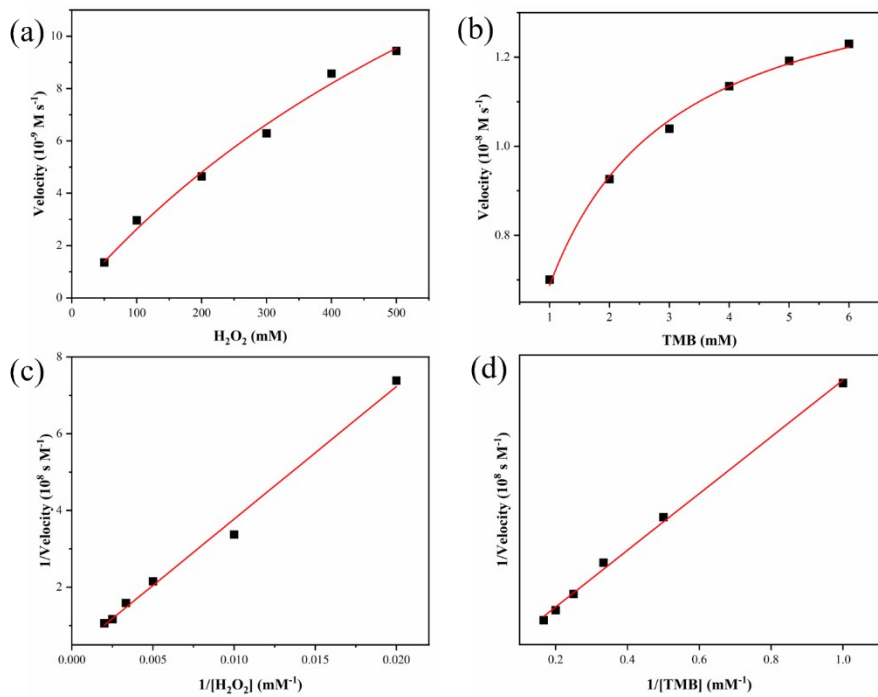


Fig. S7 Steady-state kinetics of Ni-CN nanozyme. (a and b) Michaelis–Menten curves fit for varied concentrations of H_2O_2 with fixed concentration of TMB, and varied concentrations of TMB with fixed concentration of H_2O_2 . The Lineweaver–Burk plots for various concentrations of (c) H_2O_2 and (d) TMB.

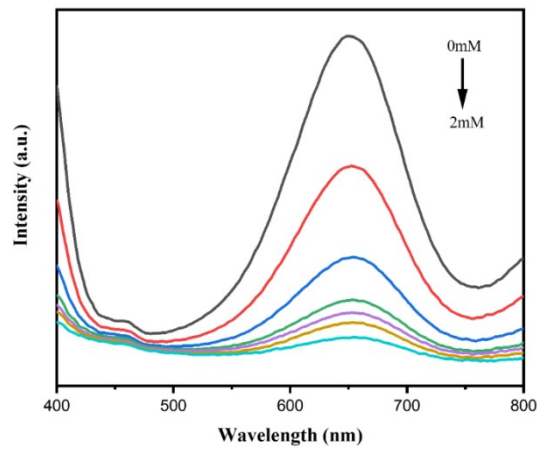


Fig. S8 The effect of •OH scavenger thiourea with different concentrations on the absorbance of TMB + H₂O₂ + Fe/Ni-CN reaction system.

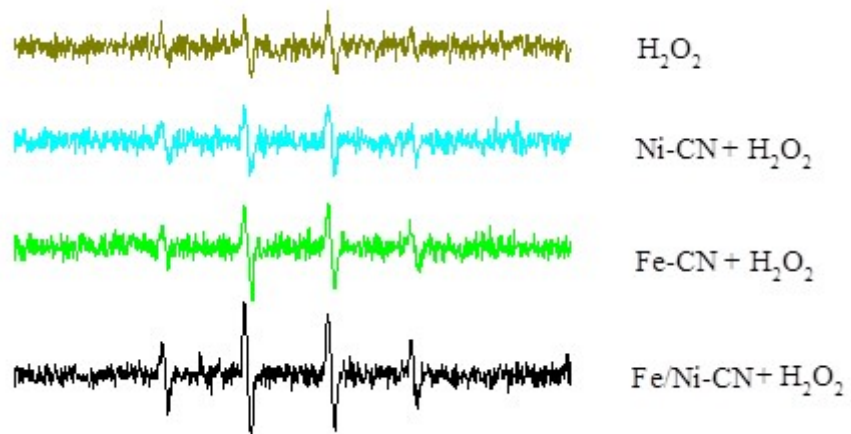


Fig. S9 The effects of Fe-CN, Ni-CN and Fe/Ni-CN on the formation of hydroxyl radical detected by ESR.

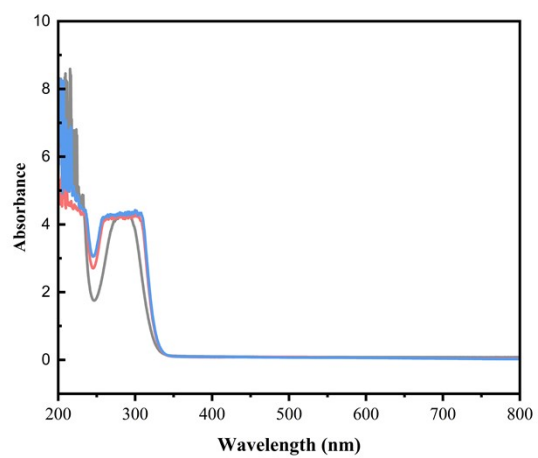


Fig. S10 The absorption spectra of dyed hair extract solutions with addition of TMB/H₂O₂. (blue: blank , red: hair dye 1, gray: hair dye 2).

Table S1. BET surface areas and pore volumes of catalysts.

Samples	S_{BET} (m ² /g)	pore volume (cm ³ /g)
CN	76.04	0.2571
Ni-CN	91.61	0.3245
Fe-CN	86.32	0.3156
Fe/Ni-CN	121.86	0.4611

Table S2. Comparison of kinetic parameters of different nanozymes.

Nanozyme	[E] $\mu\text{g/ml}$	Substrate	K_m (mM)	V_{\max} (M s^{-1})	Reference
Fe/Ni-CN	10	TMB	0.052	7.43×10^{-8}	
		H_2O_2	6.350	17.60×10^{-8}	
Fe-CN	10	TMB	0.066	7.36×10^{-8}	This work
		H_2O_2	33.15	9.82×10^{-8}	
Ni-CN	10	TMB	1.05	1.43×10^{-8}	
		H_2O_2	422	3.1×10^{-8}	
Cu NPs/g- C_3N_4	150	TMB	0.389	5.84×10^{-7}	¹
		H_2O_2	9.270	3.84×10^{-7}	
MIL-101(Fe)	20	TMB	0.585	10.038×10^{-8}	²
		H_2O_2	0.043	5.138×10^{-8}	
Co-g- C_3N_4 -2	100	TMB	0.113	8.64×10^{-8}	³
		H_2O_2	318.58	9.46×10^{-8}	
MoS ₂ @CNN S(30)	120	TMB	0.117	3.03×10^{-8}	⁴
		H_2O_2	0.602	3.15×10^{-8}	
Fe_3O_4	40	TMB	0.098	3.44×10^{-8}	⁵
		H_2O_2	154	9.78×10^{-8}	
PMCS	100	TMB	0.224	12.66×10^{-8}	⁶
		H_2O_2	40.160	12.15×10^{-8}	
HRP	1×10^{-3}	TMB	0.430	10×10^{-8}	⁷
		H_2O_2	3.700	8.70×10^{-8}	

Table S3. Calculated energies of the reaction pathway for different catalysts.

nanozyme	Free energy(ev)				
	E _{b, 1}	E _{b, 2}	E _{b, 3}	E _{b, 4}	E _{b, 5}
Fe/Ni-CN	0.35	-2.23	-1.77	-2.71	-3.59
Fe-CN	0.64	-2.67	-1.88	-2.86	-3.59
Ni-CN	0.77	-2.95	-1.97	-3.05	-3.59

Table S4. Comparison of the proposed method with other reports for the detection of PPD

Materials	Method	Linear Rang (μM)	LOD (μM)	Reference
Fe/Ni-CN	Colorimetry	0.2-30	0.02	This work
ZnBNC	Colorimetry	0.3-10	0.11	⁸
Fe ₃ O ₄ /N-GQDs	Colorimetry	2-70	0.53	⁹
Fe-SAs@FNC	Colorimetry	0.2-50	0.07	¹⁰
CDs@NBD	Fluorescence	0.1-10	0.056	¹¹
HRP/NPG/GE	ECL	2-170	0.33	¹²
S-PPD-DCM	Fluorescence	0.09-9	0.05	¹³

- 1 N. Wang, Z. W. Han, H. Fan and S. Y. Ai, *RSC Advances*, 2015, **5**, 91302-91307.
- 2 J. J. Guo, S. Wu, Y. Wang and M. Zhao, *Sensors and Actuators B: Chemical*, 2020, **312**, 128021.
- 3 J. S. Mu, J. Li, X. Zhao, E. C. Yang and X. J. Zhao, *RSC Adv.*, 2016, **6**, 35568-35576.
- 4 P. Ju, Y. H. He, M. Wang, X. X. Han, F. H. Jiang, C. J. Sun and C. Wu, *Nanomaterials (Basel)*, 2018, **8**, 976.
- 5 L. Z. Gao, J. Zhuang, L. Nie, J. B. Zhang, Y. Zhang, N. Gu, T. H. Wang, J. Feng, D. L. Yang, S. Perrett and X. Y. Yan, *Nat. Nanotechnol.*, 2007, **2**, 577-583.
- 6 B. L. Xu, H. Wang, W. W. Wang, L. Z. Gao, S. S. Li, X. T. Pan, H. Y. Wang, H. L. Yang, X. Q. Meng, Q. W. Wu, L. R. Zheng, S. M. Chen, X. H. Shi, K. L. Fan, X. Y. Yan and H. Y. Liu, *Angew Chem Int Ed Engl*, 2019, **58**, 4911-4916.
- 7 Y. Chen, H. Zou, B. Yan, X. J. Wu, W. W. Cao, Y. H. Qian, L. Zheng and G. W. Yang, *Adv. Sci.*, 2022, **9**, 2103977.
- 8 M. Feng, Q. Zhang, X. F. Chen, D. Deng, X. Y. Xie and X. P. Yang, *Biosens. Bioelectron.*, 2022, **210**, 114294.
- 9 B. F. Shi, Y. B. Su, L. L. Zhang, M. J. Huang, X. F. Li and S. L. Zhao, *Nanoscale*, 2016, **8**, 10814–10822.
- 10 X. F. Chen, M. Feng, X. Y. Xie, Y. Zhang, J. Zhang and X. P. Yang, *Talanta*, 2022, **246**, 123487.
- 11 W. J. Wang, J. M. Xia, X. Hai, M. L. Chen and J. H. Wang, *Environmental Science: Nano*, 2017, **4**, 1037-1044.
- 12 C. Wu, Z. Liu, H. H. Sun, X. Wang and P. Xu, *Biosens. Bioelectron.*, 2016, **79**, 843–849.
- 13 S. L. Zhang, B. F. Liu, D. Y. Hu, S. L. Zhang, Y. B. Pei and Z. J. Gong, *Anal. Chim. Acta*, 2020, **1139**, 189-197.